Renormalization flows in complex networks

Filippo Radicchi,[1,*] Alain Barrat,[2,1] Santo Fortunato,[1] and José J. Ramasco[1]

[1]*Complex Systems and Networks Lagrange Laboratory (CNLL), ISI Foundation, Turin, Italy*
[2]*CPT (CNRS UMR 6207), Luminy Case 907, F-13288 Marseille Cedex 9, France*

Complex networks have acquired a great popularity in recent years, since the graph representation of many natural, social, and technological systems is often very helpful to characterize and model their phenomenology. Additionally, the mathematical tools of statistical physics have proven to be particularly suitable for studying and understanding complex networks. Nevertheless, an important obstacle to this theoretical approach is still represented by the difficulties to draw parallelisms between network science and more traditional aspects of statistical physics. In this paper, we explore the relation between complex networks and a well known topic of statistical physics: renormalization. A general method to analyze renormalization flows of complex networks is introduced. The method can be applied to study any suitable renormalization transformation. Finite-size scaling can be performed on computer-generated networks in order to classify them in universality classes. We also present applications of the method on real networks.

I. INTRODUCTION

Many real systems in nature, society, and technology can be represented as complex networks [1–6]. Independently of their natural, social or technological origin, most networks share common topological features, like the "small-world" property [7] and a strong topological heterogeneity. The small-world property expresses the fact that the average distance between nodes, as defined in the graph-theoretical sense, is small with respect to the number of nodes, and typically grows only logarithmically with it. Networks are topologically heterogeneous in that the distributions of the number of neighbors (degree) of a node are broad, typically spanning several orders of magnitude, with tails that can often be described by power laws (hence the name "scale-free networks" [8]).

While "scale-free-ness" implies the absence of a characteristic scale for the degree of a node, it is not *a priori* clear how this can be related to the notion of self-similarity, often studied in statistical physics, and also typically related to the occurrence of power laws. In this context, several recent works have focused on defining and studying the concept of self-similarity for networks. The notion of self-similarity is related to a renormalization transformation, properly adapted to graphs, introduced by Song *et al.* [9]. The renormalization procedure is analogous to standard length-scale transformations, used in classical systems [10,11], and can be simply performed by using a box covering technique interpreted in a graph-theoretical sense. The analysis of this transformation in real networks [9] has revealed that some of them, such as the World Wide Web, social, metabolic, and protein-protein interaction networks, appear to be self-similar while others, like the Internet, do not. Self-similarity here means that the statistical features of a network remain unchanged after the application of the renormalization transformation. Many suc-

cessive papers have focused on this subject, performing the same analysis on several networks, introducing new box-covering techniques and trying to explain the topological differences between self-similar and non-self-similar networks [12–18] (for a recent review on this topic, see [19]).

In this context, the analysis of renormalization flows of complex networks [20] represents a new perspective to study block transformations in graphs. Differently from all former studies, the study of Ref. [20] is not devoted to observe the effect of a single transformation, but to analyze the renormalization flow produced by repeated iterations of the transformation. Starting from an initial network, the iteration of the renormalization procedure allows us to explore the space of network configurations just as standard renormalization is used to explore the phase space of classical systems in statistical physics [10,11]. For these reasons, the analysis of renormalization flows of complex networks represents not only an important theoretical step towards the understanding of block transformations in graphs, but also a further attempt to link traditional statistical physics and network science.

In this paper, we substantially extend the analysis presented in [20]. We perform a numerical study of renormalization flows for several computer-generated and real networks. The numerical method is applied to different renormalization transformations. For a particular class of transformations, we find that the renormalization flow leads non-self-similar networks to a condensation transition, where a few nodes attract a large fraction of all links. The main result of the paper lies in the robustness of the scaling rules governing the renormalization flow of a network: independently of the transformation, the renormalization flow of non-self-similar networks is characterized by the same set of scaling exponents, which identify a unique universality class. In contrast, the renormalization flow of self-similar networks allows to classify these networks in different universality classes, characterized by a set of different scaling exponents.

The paper is organized in the following way. In Sec. II, we describe the standard technique used in order to renormalize a network and define the renormalization flow of a graph. We then start with the analysis of renormalization

_____

*Author to whom correspondence should be addressed.
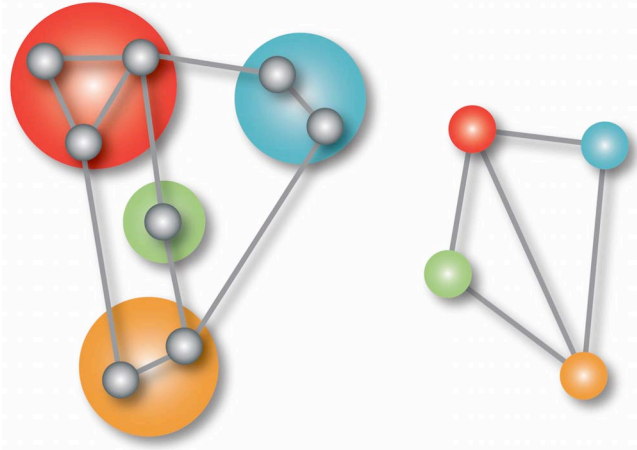f.radicchi@gmail.com

FIG. 1. (Color online) Renormalization procedure applied to a simple graph: (left) the original network is divided into boxes and the renormalized graph (right) is generated according to this tiling.

flows of different networks. In the case of computer-generated graphs, we distinguish the behavior of non-self-similar (Sec. III A) and self-similar (Sec. III B) networks. Section IV is devoted to the analysis of the renormalization flows of real complex networks. Finally, in Sec. V we summarize and comment on the results.

II. RENORMALIZING COMPLEX NETWORKS

Differently from classical systems, graphs are not embedded in Euclidean space. As a consequence, standard length-scale transformations cannot be performed on networks since measures of length have a meaning only in a graph-theoretical sense: the length of a path is given by the number of edges which compose the path; the distance between two nodes is given by the length of the (or one of the) shortest path(s) connecting the two nodes. Based on this metrics, Song *et al.* [9] proposed an original technique for renormalizing networks (see Fig. 1). Given the length of the transformation ℓ_B, their method is given by the following steps:

(i) Tile the network with the minimal number of boxes N_B; each box should satisfy the condition that all pairs of nodes within the box have distance less than ℓ_B.

(ii) Replace each box with all nodes and mutual edges inside with a supernode.

(iii) Construct the renormalized network composed of all supernodes: two supernodes are connected if in the original network there is at least one link connecting nodes of their corresponding boxes.

The former recipe represents a transformation R_{ℓ_B} applicable to any unweighted and undirected network leading to the generation of a new unweighted and undirected network, the "renormalized" version of the original one. In principle, there are many ways to tile a network and therefore the transformation R_{ℓ_B} is not invertible. Moreover, finding the best coverage of a network (i.e., the one which minimizes the number of boxes N_B) is computationally expensive: up to now, the best algorithm introduced in this context is the greedy coloring algorithm [15] (GCA), a greedy technique

TABLE I. We list the values of the scaling exponent ν and of the fixed point threshold x^* (fourth and fifth column, respectively) for all networks we consider in our numerical analysis. Computer-generated networks (specified in the second column) are divided in non-self-similar, self-similar, and perturbed self-similar (first column). The perturbation is made by rewiring a fraction $p=0.01$ of all links in the WS model and by adding a fraction $p=0.05$ or $p=0.01$ of all connections in the FM or AP networks, respectively. The third column specifies the type of transformation used to analyze the renormalization flow. We associate to each numerical value of ν and x^* its error.

Type	Network	R	ν	x^*
Non-self-similar	ER $\langle k \rangle = 2$	$r_B = 1$	2.0(1)	0.059(1)
		$\ell_B = 2$	2.0(1)	0.15(1)
		$r_B = 2$	2.0(1)	0
		$\ell_B = 3$	2.0(1)	0
	BA $m = 3$	$r_B = 1$	2.0(1)	0.098(2)
		$\ell_B = 2$	2.0(1)	0.245(5)
		$r_B = 2$	2.0(1)	0
		$\ell_B = 3$	2.0(1)	0
Self-similar	WS $\langle k \rangle = 4$	$r_B = 1$	1.0(1)	0
		$\ell_B = 2$	1.0(1)	0
		$\ell_B = 3$	1.0(1)	0
	FM $e = 0.5$	$r_B = 1$	2.2(1)	0
		$\ell_B = 2$	2.2(1)	0
		$\ell_B = 3$	1.0(1)	0
	AP	$\ell_B = 2$	4.8(2)	0
		$\ell_B = 3$	1.0(1)	0
Perturbed self-similar	WS $\langle k \rangle = 4$	$r_B = 1$	2.0(1)	0.004(2)
		$\ell_B = 3$	2.0(1)	0
	FM $e = 0.5$	$r_B = 1$	2.1(1)	0.118(2)
		$\ell_B = 3$	2.0(1)	0
	AP	$r_B = 1$	2.0(1)	0.045(2)
		$\ell_B = 2$	2.0(1)	0.05(1)
		$\ell_B = 3$	2.0(1)	0

inspired by the mapping of the problem of tiling a network to node coloring, a well known problem in graph theory [21]. An analogous technique, leading to a qualitatively and quantitatively similar transformation R_{r_B}, is random burning (RB) [14]. In RB boxes are spheres of radius r_B centered at some seed nodes, so that the maximal distance between any two nodes within a box does not exceed $2r_B$. Nodes in boxes defined through the transformation R_{r_B} satisfy the condition defining boxes of the transformation R_{ℓ_B}, for $\ell_B = 2r_B + 1$. However, the search for minimal box coverage is much more effective for the GCA than for RB, and this may occasionally yield different results, as we shall see.

The strict meaning of self-similarity is that any part of an object, however small, looks like the whole [22]. Similarly, complex networks are self-similar if their statistical properties are invariant under a proper renormalization transformation. Song *et al.* [9] have shown that the degree distribution
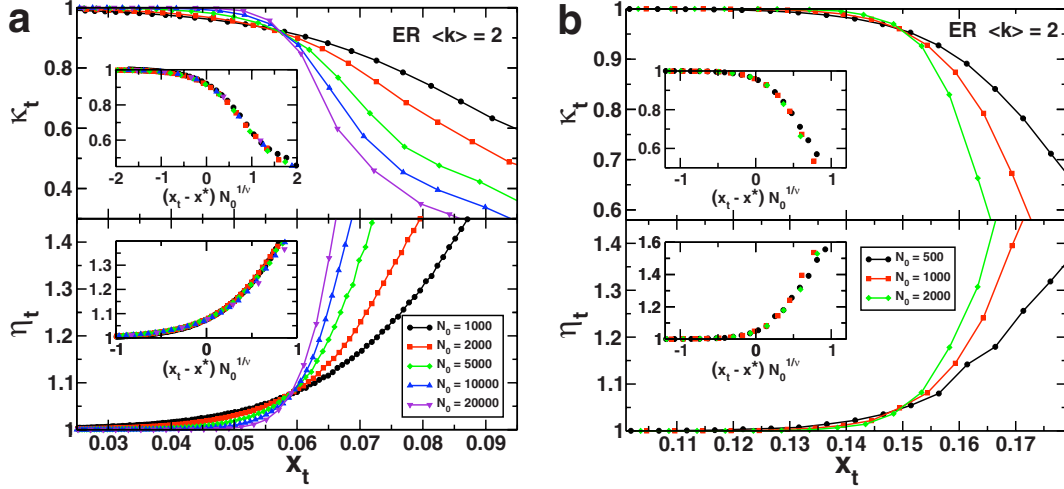
FIG. 2. (Color online) Study of renormalization flows on the ER model with $\langle k \rangle = 2$. The box covering has been performed by using RB with $r_B = 1$ (a) and GCA with $\ell_B = 2$ (b). The figures display κ_t (a, b top) and η_t (a, b bottom) as a function of the relative network size x_t. The insets display the scaling function of the variable $(x_t - x^*)N_0^{1/\nu}$ for κ_t and η_t. Here the scaling exponent $\nu = 2$ in both cases. Note that the flow of the renormalization procedure goes from larger (right on the x axis) to smaller values (left) of x_t.

of several real networks remains unchanged if a few iterations of the renormalization transformation are performed. Moreover, when this feature is verified, the number of boxes N_B needed to tile the network for a given value of the length parameter ℓ_B decreases as a power law as ℓ_B increases:

$$N_B(\ell_B) \sim \ell_B^{-d_B}. \tag{1}$$

The exponent d_B is called, in analogy with classical systems, the fractal exponent of the network [22]. This property has been verified for several real networks in various studies [9,12,14]. On the other hand, not all real networks are self-similar, i.e., Eq. (1), and the invariance of the degree distribution do not hold for them. For consistency, these networks are called non-self-similar.

In contrast to former studies which mostly dealt with a single step of renormalization, we are interested here in analyzing renormalization *flows* of complex networks, i.e., the outcome of repeated iterations of the renormalization procedure described above. Starting from a graph G_0, with N_0 nodes and E_0 edges, we indicate as G_t (with N_t nodes and E_t edges) the network obtained after t iterations of the transformation R:

$$G_1 = R(G_0), \quad G_2 = R(G_1) = R^2(G_0), \dots$$

$$\dots, G_t = R(G_{t-1}) = \cdots = R^t(G_0). \tag{2}$$

Note that in Eq. (2) we have suppressed the subscript ℓ_B (or r_B) for clarity of notation. In our analysis, we follow the flow by considering several observables. We mainly focus on the variables

$$\kappa_t = K_t/(N_t - 1), \tag{3}$$

where K_t is the largest degree of the graph G_t, and

$$\eta_t = E_t/(N_t - 1), \tag{4}$$

which is basically the average degree of the graph G_t divided by 2. κ_t and η_t can assume nontrivial values in any graph,

excluding trees (for which $\eta_t = 1$, $\forall t$). We monitor also the fluctuations of the variable κ_t along the flow by measuring the susceptibility

$$\chi_t = N_0(\langle \kappa_t^2 \rangle - \langle \kappa_t \rangle^2), \tag{5}$$

where $\langle \cdot \rangle$ denotes averages taken over different realizations of the covering algorithm. Moreover, we consider other quantities like the average clustering coefficient C_t [7]. All these observables are monitored as a function of the relative network size $x_t = N_t/N_0$, which is a natural way of following the renormalization flow of the variables under study.

III. COMPUTER-GENERATED NETWORKS

We first consider artificial networks. In the case of computer-generated networks, it is in fact possible to control the size N_0 of the initial graph G_0 and to perform the well known finite-size scaling analysis for the renormalization flow. For every computer-generated graph and every transformation R, we find that the observable κ_t obeys a relation of the type

$$\kappa_t = F[(x_t - x^*)N_0^{1/\nu}], \tag{6}$$

where $F(\cdot)$ is a suitable function depending on the starting network and the particular transformation used. Analogous scaling relations hold for the other observables (η_t and C_t) we considered. The susceptibility χ_t needs an additional exponent γ since it obeys a relation of the type $\chi_t = N_0^{\gamma/\nu} G[(x_t - x^*)N_0^{1/\nu}]$, with $G(\cdot)$ a suitable scaling function. In general, the scaling exponent ν does not depend on the particular transformation R used to renormalize the network, but depends on the starting network G_0: we always obtain $\nu = 2$ for any non-self-similar network (Sec. III A) and values of ν depending on the initial network in the case of self-similar graphs (Sec. III B). On the other hand, we obtain $x^* = 0$ in all cases, except for the particular transformations obtained for
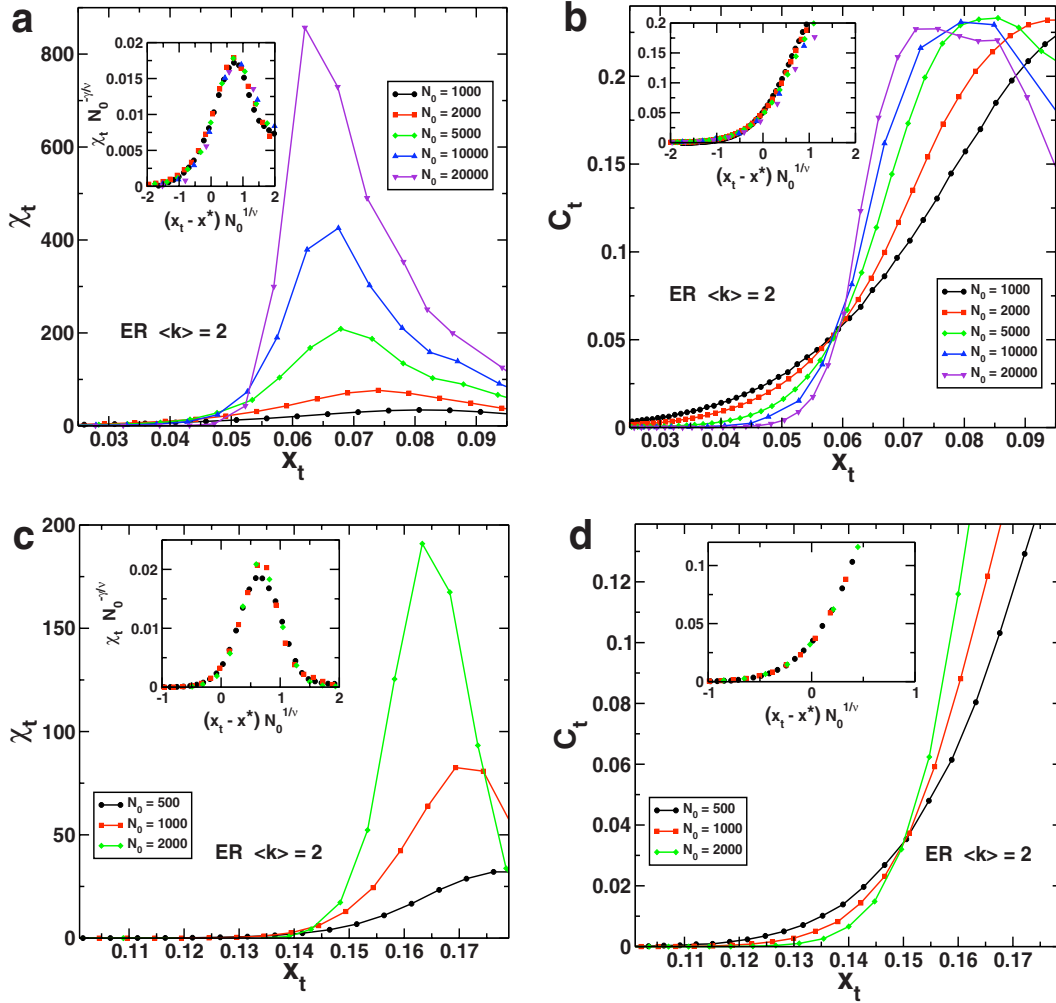
FIG. 3. (Color online) Study of renormalization flows on ER model with $\langle k \rangle = 2$. The box covering has been performed by using RB with $r_B = 1$ (a, b) and GCA with $\ell_B = 2$ (c, d). The figures display the susceptibility χ_t (a, c) and the average clustering coefficient C_t (b, d) as a function of the relative network size x_t. The insets display the scaling function of the variable $(x_t - x^*) N_0^{1/\nu}$ for χ_t and C_t. Here the scaling exponent $\nu = 2$ and the susceptibility exponent $\gamma = \nu$ in all cases.

$r_B = 1$ and $\ell_B = 2$ on non-self-similar networks (Sec. III A 1). In the next sections, we show our numerical results, obtained from the analysis of renormalization flows of computer-generated networks, distinguishing between the various cases. All values of ν and x^* are listed in Table I. We emphasize the importance of the fact that the exponent ν is able to classify artificial networks in different universality classes.

A. Non-self-similar networks

We consider several computer-generated networks for which Eq. (1) does not hold. Equation (6) is able to describe the renormalization flows of any of these network models. The scaling exponent $\nu = 2$ identifies a single universality class for all these models. The only difference is given by the finite value of $x^* > 0$ obtained when renormalization is performed with $\ell_B = 2$ or $r_B = 1$ (Sec. III A 1). Instead, for $\ell_B > 2$ and $r_B > 1$ we always obtain $x^* = 0$ (Sec. III A 2).

1. $r_B = 1$, $\ell_B = 2$

For $r_B = 1$ or $\ell_B = 2$, the transformation R has a particular behavior. In the case of GCA and $\ell_B = 2$, at each stage of the

renormalization flow, the boxes in which the network is tiled have the peculiarity to be fully connected subgraphs or *cliques* [23]. In the case of renormalization performed with RB and $r_B = 1$, spheres are compact subgraphs composed only of neighbors of the selected seed nodes. In both cases, at each stage of the renormalization flow, the contraction of the network is much slower if compared with the same transformations run for higher values of ℓ_B or r_B.

In Fig. 2, we show some numerical results obtained following the renormalization flow of the Erdös-Rényi (ER) [24] model with average degree $\langle k \rangle = 2$. For both algorithms used for renormalizing the networks, we clearly see a point of intersection between all the curves occurring at a particular value $x^* > 0$. Interestingly, the same values of ν and x^* hold also for the susceptibility χ_t and the average clustering coefficient C_t. Numerical results for both quantities and their relative scaling are reported in Fig. 3.

The same behavior is observed for all the non-self-similar networks that we have studied. To mention a few, we performed numerical simulations also on the Barabási-Albert (BA) model [8] and its generalization given by scale-free
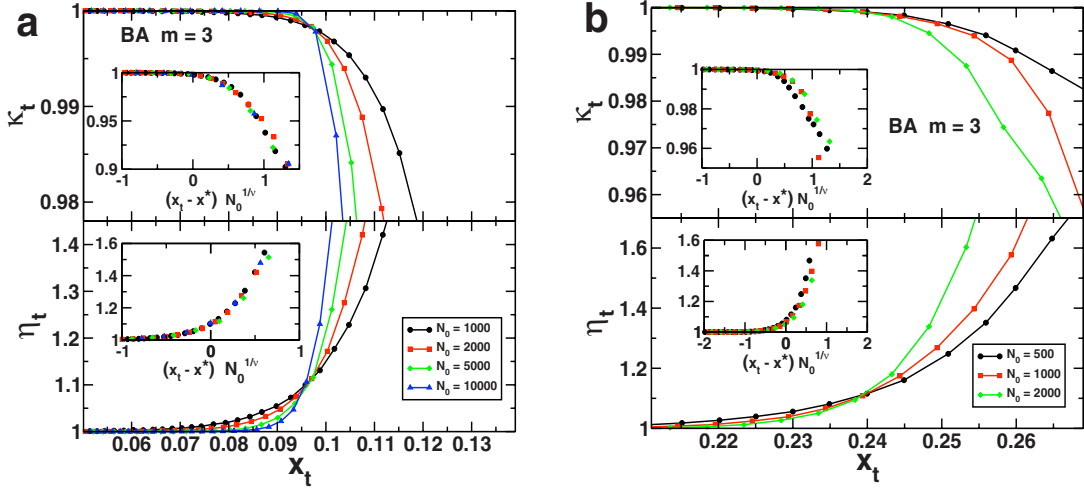
FIG. 4. (Color online) Study of renormalization flows on the BA model with $2m=\langle k \rangle=6$ (m indicates the number of connections introduced by each node during the construction of the BA model). The box covering has been performed by using RB with $r_B=1$ (a) and GCA with $\ell_B=2$ (b). The figures display the variables κ_t (a,b top) and η_t (a,b bottom) as a function of the relative network size x_t. The insets display the scaling function of the variable $(x_t - x^*)N_0^{1/\nu}$ for κ_t and η_t. Here the scaling exponent $\nu=2$ in both cases.

networks generated with linear preferential attachment [25]. We report in Fig. 4 the numerical results obtained for the BA model: the quantities κ_t and η_t are shown as a function of the renormalization flow's variable x_t. Again, a clear crossing point $x^*>0$ can be seen in this case. More importantly, both variables κ_t and η_t obey Eq. (6) with $\nu=2$.

The existence of a nonvanishing x^* is a peculiarity of the renormalization obtained for $\ell_B=2$ and $r_B=1$: $x^*>0$ implies the existence of a special stable fixed point, which holds in the limit of infinite network size. The fixed point is reached in a number of iterations which scales logarithmically with the initial size of the network, while the number of renormalization stages needed to reach any $x_t<x^*$ diverges almost linearly with the initial system size (see Fig. 5). Interestingly, the fixed point statistically corresponds to the same topologi-

cal structure, independently of the topology of the initial network (see Fig. 6). This particular fixed point is a graph where a few nodes attract a large fraction of all links [i.e., $\kappa_t(x^*) \approx 1$]; such hub nodes have degrees which are distributed according to a power law [see Fig. 6(a)]. Moreover, the network obtained at the fixed point is composed of nodes with clustering coefficient (C) and average degree of the neighbors (k_{nn}) which decrease as a power law as the degree of the node increases [see Figs. 6(b) and 6(c) respectively]. Figure 6(d) is a graphical representation of the graph obtained at x^* when starting from an ER network with $N_0=30\,000$. The presence of many starlike structures gives an explanation of the results described above (Fig. 5): for $r_B=1$, the center of the first chosen box will be with high probability a low-degree node ("leaf" in the figure), so the box will include
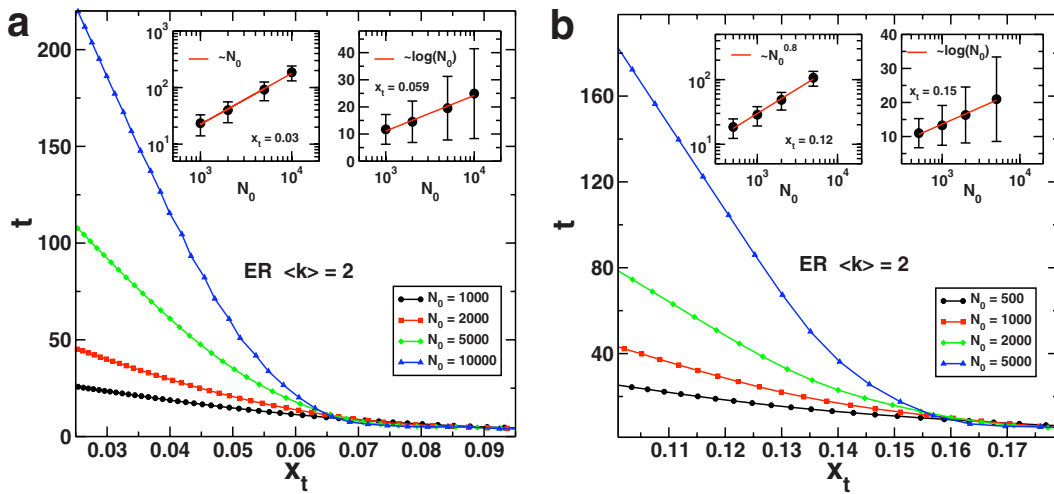

FIG. 5. (Color online) Study of renormalization flows on the ER model with $\langle k \rangle=2$. The box covering has been performed by using RB with $r_B=1$ (a) and GCA with $\ell_B=2$ (b). The figures display the number of iterations t as a function of the relative network size x_t. The fixed point [i.e., $x_t=x^*=0.059$ (RB), 0.015 (GCA)] is reached in a number of renormalization steps growing logarithmically with the initial system size N_0 (see the insets on the right in each figure). In contrast, the number of stages needed to go out from the fixed point (i.e., to reach a given $x_t<x^*$) grows as a power of N_0 (see the insets on the left in each figure).
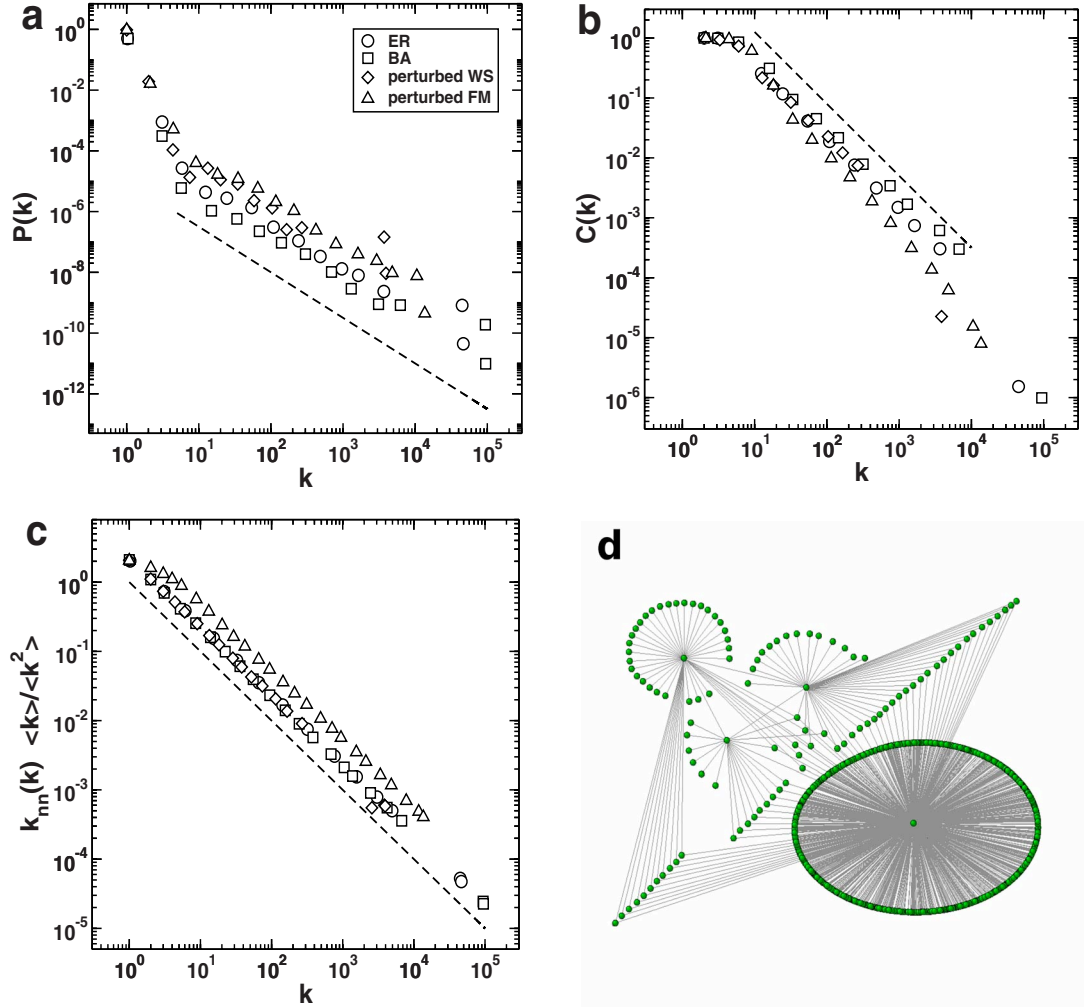
FIG. 6. (Color online) Statistical properties of the fixed point in the case of computer-generated networks. Renormalization has been performed by using GCA with $\ell_B=2$. Initial network sizes are $N_0=10^6$ for the ER model, $N_0=10^6$ for the BA model, $N_0=10^6$ for the Watts-Strogatz (WS) model (with ratio of rewired links $p=0.01$), and $N_0=156\ 251$ for the fractal model (FM), with ratio of added connections $p=0.05$. Dashed lines have slopes -1.5 in (a), -1.2 in (b), and -1 in (c). (d) The graphical representation of the fixed point has been obtained by starting from an ER model with $N_0=30\ 000$ and $\langle k\rangle=2$.

only a low-degree node and the attached hub, and the other low-degree nodes (the other leaves of the star) will need one box each. This is why N_t decreases very slowly. Renormalization steps with "small" boxes ($r_B=1$ or $\ell_B=2$) make it therefore "difficult" or "slow" to modify appreciably such structures.

2. $r_B>1$, $\ell_B>2$

Renormalization flows with $\ell_B>2$ and $r_B>1$ have been discussed in [20], and we present some additional results in Fig. 7. The renormalization flows of non-self-similar computer-generated networks still obey Eq. (6) with $\nu=2$, and the main difference with respect to the particular cases $\ell_B=2$ and $r_B=1$ consists in the value of x^*, which is now $x^*=0$. As usual in statistical physics, however, the precise value of the threshold is less relevant than the value of the exponents describing the flow. In this respect, the robustness of the value $\nu=2$ strikingly shows that all non-self-similar

artificial networks can be classified as belonging to a unique universality class.

B. Self-similar networks

Let us now consider computer-generated models which satisfy Eq. (1). For all these models, we find that Eq. (6) still holds. In strong contrast with non-self-similar networks, the value of the scaling exponent ν now depends on the particular network analyzed and on the specific renormalization transformation. Moreover, each self-similar model is a fixed point of the renormalization flow since the statistical properties of the network are unchanged if iterated renormalization transformations are applied to the network.

As a prototype of computer-generated self-similar network, we consider the fractal model (FM) introduced by Song *et al.* [13]. The FM is self-similar by design, as it is obtained by inverting the renormalization procedure. At each step, a node turns into a star, with a central hub and several nodes with degree 1. Nodes of different stars can then be
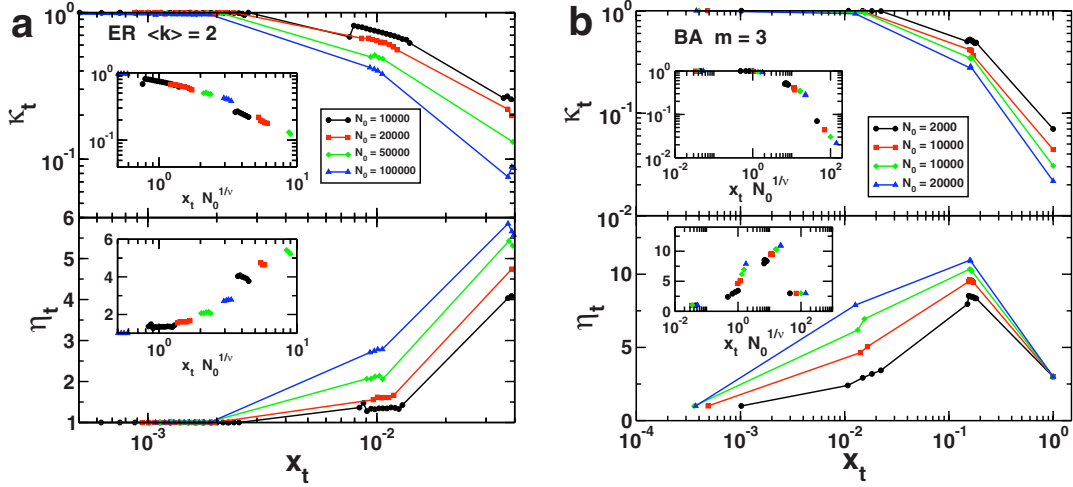
FIG. 7. (Color online) Study of renormalization flows on non-self-similar artificial graphs. Renormalization has been performed by using GCA with $\ell_B=3$. The figures display the variables κ_t (a,b top) and η_t (a,b bottom) as a function of the relative network size x_t, for the renormalization flow of an ER model with $\langle k \rangle=2$ (a) and a BA model with $2m=\langle k \rangle=6$ (b). The insets display the scaling function of the variable $(x_t-x^*)N_0^{1/\nu}$ for κ_t and η_t. Here the scaling exponent is $\nu=2$ in both cases.

connected in two ways: with probability e one connects the hubs with each other, with probability $1-e$ a nonhub of a star is connected to a nonhub of the other. The resulting network is a tree with power law degree distribution, the exponent of which depends on the probability e.

In the case of the FM network it is possible to derive the scaling exponent ν, by inverting the construction procedure of the graph. In this way one recovers graphs with identical structure at each renormalization step and one can predict how κ_t, for instance, varies as the flow progresses. Since we are interested in renormalizing the graph, our process is the time-reverse of the growth described in [13], and is characterized by the following relations:

$$N_{t-1} = nN_t,$$

$$k_{t-1} = sk_t,$$

$$\beta = 1 + \frac{\ln n}{\ln s}, \qquad (7)$$

where n and s are time-independent constants determining the value of the degree distribution exponent β of the network. Here N_t and k_t are the number of nodes and a characteristic degree of the network at step t of the renormalization; we choose the maximum degree K_t. The initial network has
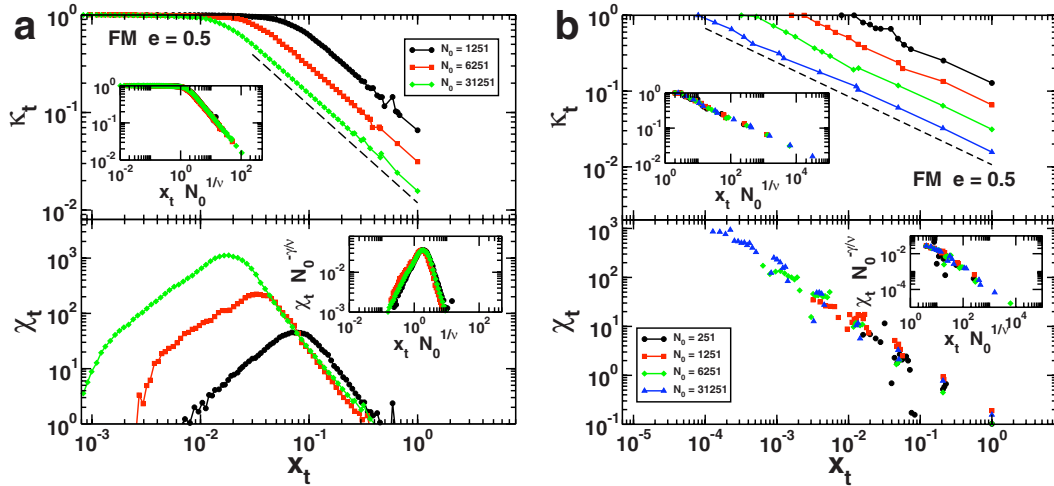

FIG. 8. (Color online) Study of renormalization flows on self-similar artificial graphs. The box covering has been performed by using RB with $r_B=1$ (a) and GCA with $\ell_B=3$ (b). The graph is an FM network with $e=0.5$, where e is the probability for hub-hub attraction [13]. The figures display κ_t (a,b, top), and χ_t (a,b, bottom) as a function of the relative network size x_t. The scaling function of the variable $(x_t-x^*)N_0^{1/\nu}$ for κ_t and χ_t is displayed in the insets. We find that the two box covering techniques yield different exponent values: $\nu=2.2$ (RB) and $\nu=1$ (GCA). The dashed lines indicate the predicted behavior of the scaling function. In (a) the exponent of the power law decay for the scaling function is -1, independently of the exponent β of the degree distribution of the initial graph; in (b) instead the scaling function decays with an exponent $-(\beta-2)/(\beta-1)=-0.45$. We still find $\gamma=\nu$ for both transformations.
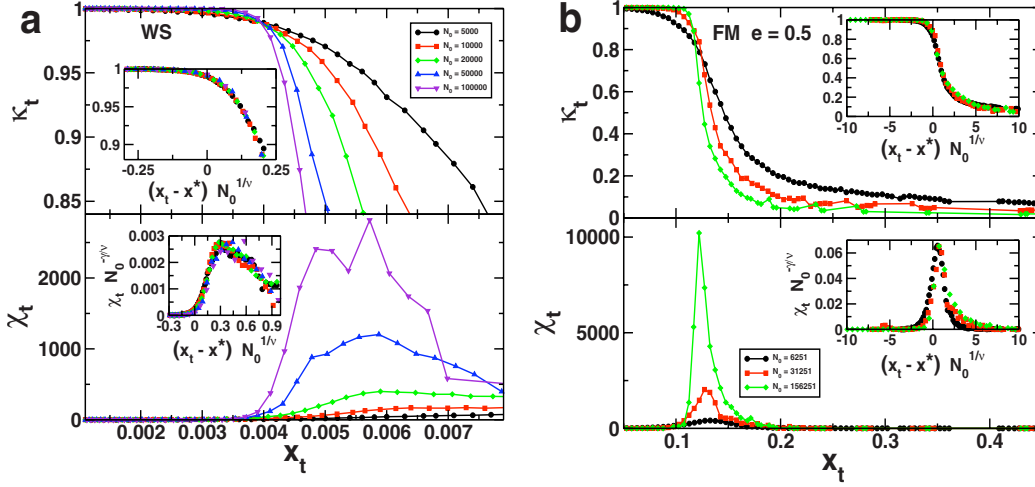
FIG. 9. (Color online) Effect of a small random perturbation on renormalization flows. The box covering has been performed by using RB with $r_B=1$. (a) WS network with $\langle k \rangle = 4$ and a fraction $p=0.01$ of randomly rewired links. (b) FM network with $e=0.5$ and a fraction $p=0.05$ of added links. The figures display κ_t (a,b, top), and χ_t (a,b, bottom) as a function of the relative network size x_t. Comparing with Fig. 8(a), we see that the transformation yields a crossing of the κ_t curves for the FM networks. The crossing appears also for the WS networks, while in the unperturbed case the κ_t curves do not cross since these networks correspond to linear chains (trivially self-similar). The exponents are now very different from the unperturbed case: we recover $\nu=2$. The relation $\gamma=\nu$ seems to hold here as well.

size N_0 and shrinks due to box-covering transformations. In this case, for the variable κ_t one obtains

$$\kappa_t \sim \frac{K_t}{N_t} = \frac{K_0}{N_0}\left(\frac{s}{n}\right)^{-t} = \frac{K_0}{N_0}\left(\frac{N_t}{N_0}\right)^{-(\beta-2)/(\beta-1)} = \frac{K_0}{N_0}x_t^{-(\beta-2)/(\beta-1)}$$
$$\sim (N_0 x_t)^{-(\beta-2)/(\beta-1)}, \tag{8}$$

where we used $s=n^{1/(\beta-1)}$, $N_t/N_0=n^{-t}$, and $K_0 \sim N_0^{1/(\beta-1)}$, derived from Eqs. (7). We see that the scaling exponent $\nu=1$ is obtained for any value of the exponent β. From Eq. (8) we actually get the full shape of the scaling function, that is, a power law: our numerical calculations confirm this prediction [see Fig. 8(b)]. We remark that this holds only because one has used precisely the type of transformation that inverts the growth process of the fractal network. This amounts to applying the GCA with $\ell_B=3$, as we did Fig. 8(b).

If we consider instead the renormalization procedure defined by RB with $r_B=1$ (or by GCA with $\ell_B=2$), the centers of the boxes will be mostly low degree nodes, as discussed above. Hubs are thus included in boxes only as neighbors of low degree nodes and, as a consequence, the supernode corresponding to a box with a large hub inside will have a degree which is essentially the same as the degree of the hub before renormalization. It is therefore reasonable to assume that $K_t \sim K_0$, and we get

$$\kappa_t \sim \frac{K_t}{N_t} \sim \frac{K_0}{N_t} \sim \frac{N_0^{1/(\beta-1)}}{N_t} = (N_0^{(\beta-2)/(\beta-1)}x_t)^{-1} \tag{9}$$

which is again a scaling function of the variable $N_0^{1/\nu}x_t$, with $\nu=(\beta-1)/(\beta-2)$, as we found numerically [see Fig. 8(a)].

Qualitatively similar numerical results can be shown also for other self-similar models of networks: unperturbed Watts-Strogatz (WS) model [7] (i.e., one-dimensional lattice), hierarchical model [27] and the Apollonian (AP) network model [28] (see Table I).

C. Effect of small perturbations on self-similar networks

Self-similar objects correspond by definition to fixed points of the transformation. To study the nature of these fixed points, we have repeated the analysis of the renormalization flows for the self-similar networks considered, but *perturbed* by a small amount of randomness, through the addition or rewiring of a small fraction p of links. The results are shown in Fig. 9 for WS small-world networks, which are simply linear chains (trivially self-similar) perturbed by a certain amount of rewiring [7], and FM networks with randomly added links. In both cases we recover the behavior observed for non-self-similar graphs, with a scaling exponent $\nu=2$ (this holds for all values of r_B or ℓ_B investigated, see also [20]). This clearly implies that the original self-similar fixed points are unstable with respect to disorder in the connections, and highlights once again the robustness of the exponent value $\nu=2$. Furthermore, the statistical properties of the fixed point reached at x^*, when it exists (i.e., for $r_B=1$ or $\ell_B=2$) are again the same as those obtained starting from non-self-similar networks (see Fig. 6). For these particular renormalization flows (for $r_B=1$ or $\ell_B=2$), the picture obtained is therefore a global flow towards the structure depicted in Fig. 6, with isolated unstable fixed points given by the artificial self-similar graphs.

IV. REAL NETWORKS

For real-world networks, a finite-size scaling analysis is not available because of the uniqueness of each sample. On the other hand, it is still possible to apply repeatedly the renormalization transformation and to study the evolution of the network properties (a similar numerical study has been performed also in [29]). In Fig. 10, we measure some basic statistical properties of two real networks along the renormalization flow. We consider the actor network [8], a graph
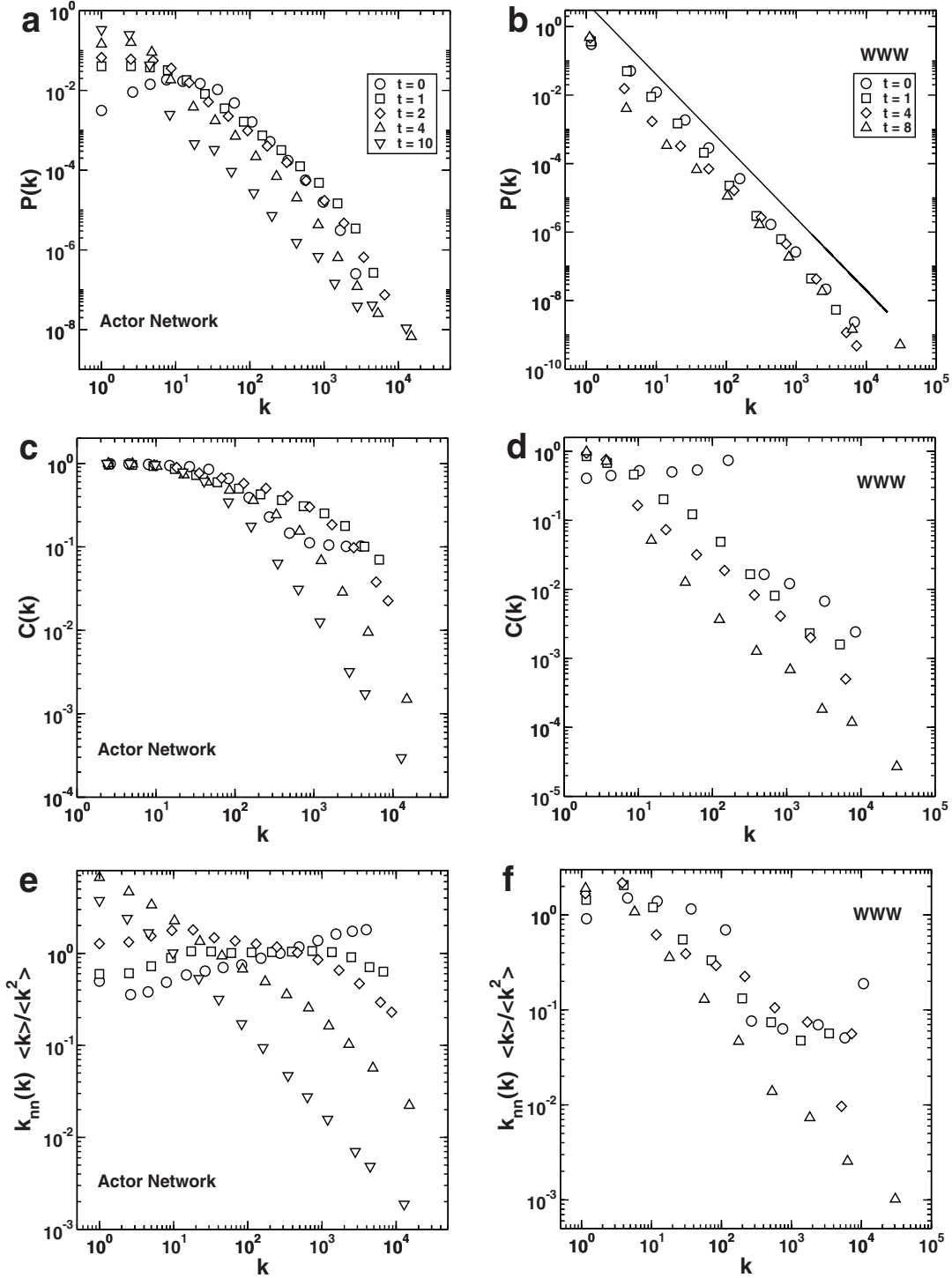
FIG. 10. (Color online) Statistical properties of real networks after t steps of renormalization. We consider two examples: a network of 392 340 actors, where nodes are connected if the corresponding actors were cast together in at least one movie [8] (a, c, and e); the link graph of the World Wide Web, consisting of 325 729 Web pages of the domain of the University of Notre Dame (Indiana, USA) and of their mutual hyperlinks [26] (b, d, and f). The box covering was performed with the GCA ($\ell_B=2$), but the results hold as well for other transformations. The clustering spectrum and the degree correlation pattern change drastically already after a single transformation. In particular, the actor network displays assortativity, but after two transformations it becomes disassortative. The solid line in (b) has slope −2.1.

constructed from the Internet Movie Database [32] where nodes are connected if the corresponding actors were cast together in at least one movie, and the link graph of the Web pages of the domain of the University of Notre Dame (Indiana, USA) [26]. Both networks have been claimed to be

self-similar, since Eq. (1) holds for both of them [9]. On the one hand, the degree distributions $P(k)$ are only slightly affected by the renormalization transformation, and retain their main characteristics even after several stages of renormalization [in particular for the Web graph, see Fig. 10(b)]. This
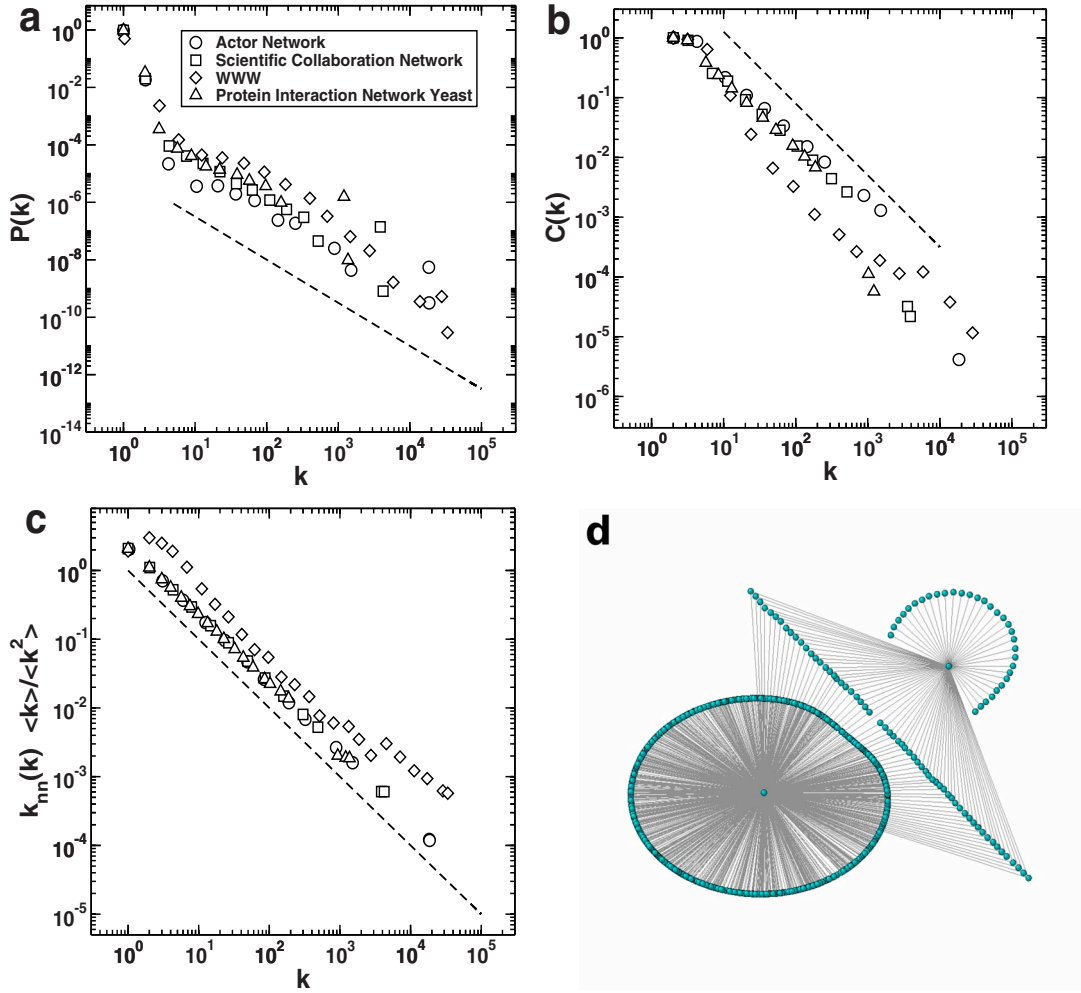
FIG. 11. (Color online) Statistical properties of the "fixed point" in the case of real networks. Renormalization has been performed by using GCA with $\ell_B = 2$. The properties of the networks are measured after a certain number (less than 10) of renormalization steps. Dashed lines have the same slopes as those appearing in Fig. 6. The real networks considered in this figure are the actor network [8], the scientific collaboration network [30], the network of Web pages of the domain of the University of Notre Dame [26], and the protein-protein interaction network of the yeast *Saccharomyces cerevisae* [31]. (d) The graphical representation of the fixed point has been obtained by starting from the protein-protein interaction network of the yeast.

first result points towards an effective self-similarity of $P(k)$ under the action of the renormalization flow. The degree distribution by itself is, however, not enough to characterize complex networks, since many different topologies can correspond to the same $P(k)$. Important information is in particular encoded in the clustering coefficient spectrum $C(k)$, defined as the average clustering coefficient of nodes of degree k, and in the average degree of the neighbors of nodes of degree k, $k_{nn}(k)$, which is a measure of the degree correlations between nearest neighbors in the graph. In this context, Figs. 10(c)–10(f) show that even a single renormalization transformation induces large changes in these quantities. In this respect, the apparent self-similarity exhibited by the degree distribution does not extend to higher order correlation patterns.

Interestingly, in the case $r_B = 1$ or $\ell_B = 2$, the iteration of the renormalization transformation leads all real networks investigated [either self-similar or not, as defined by Eq. (1)] towards the same kind of structure (illustrated in Fig. 6) which is reached by non-self-similar artificial networks (see

Fig. 11). Note that, for real networks, no change in the initial size can be performed, so we simply show the structure obtained after a few steps of renormalization, which remains stable for many steps due to the peculiarity of the case $r_B = 1$ or $\ell_B = 2$, as explained above.

All these results allow us to discuss the exact self-similarity of real-world networks: as we have seen in the case of computer-generated self-similar networks, all fixed points correspond to strongly regular topologies and minimal perturbations are enough to break the picture of self-similarity. Since randomness is an unavoidable element in real complex networks, exact self-similarity should not be observed in them. The randomness of their topology is amplified when renormalization is iterated. Real-world networks which are self-similar according to Eq. (1) could, however, *a priori* be arbitrarily close to an actual fixed point of the renormalization. This actually raises the important issue of defining and measuring a distance in the space of networks. However, Fig. 10 shows that few renormalization steps (often a single one) are enough to substantially modify

the network structure in our examples, so that it seems to us hard to sustain that they are close to a fixed point.

V. SUMMARY AND CONCLUSIONS

In this paper we have presented a detailed analysis of the method, introduced in [20], to study renormalization flows of complex networks. The method is applied using the two most popular techniques for network renormalization: greedy coloring [13] and random burning [14]. Independently of the algorithm, we have shown that a simple scaling rule [i.e., Eq. (6)] is able to describe the renormalization flow of any computer-generated network. A single scaling exponent ν is needed in order to classify networks in universality classes: all non-self-similar networks belong to the same universality class characterized by $\nu = 2$; self-similar networks, on the other hand, belong to other universality classes, generally identified by values of the scaling exponent ν different from 2. Self-similar networks represent by definition fixed points of the renormalization transformation, since the statistical properties of these networks remain invariant after renormalization. They are actually unstable fixed points of the renormalization transformation: minimal random perturbations are indeed able to lead the flow out of these fixed points. The numerical study presented here confirms and extends the validity of the results already anticipated in [20].

In addition, we have performed an analysis of the effect of the iterated renormalization transformation on real networks. Unfortunately, the same technique, introduced in [20], cannot be directly applied to real networks. In this case, in fact, a finite-size scaling analysis cannot be performed since any real network has a fixed size. Nevertheless, the usual simple measures of the network structure, taken after a few iterations of renormalization, reveal that the transformation modifies the topological properties of the network. Furthermore, the repeated renormalization of real networks produces flows converging to the same fixed point structure, when it exists, as the one found in the case of computer-generated non-self-similar networks.

[1] R. Albert and A.-L. Barabási, Rev. Mod. Phys. **74**, 47 (2002).

[2] M. E. J. Newman, SIAM Rev. **45**, 167 (2003).

[3] S. N. Dorogovtsev and J. J. F. Mendes, *Evolution of Networks: From Biological Nets to the Internet and WWW* (Oxford University Press, Oxford, 2003).

[4] R. Pastor-Satorras and A. Vespignani, *Evolution and Structure of the Internet: A Statistical Physics Approach* (Cambridge University Press, Cambridge, England, 2004).

[5] S. Boccaletti, V. Latora, Y. Moreno, M. Chavez, and D. U. Hwang, Phys. Rep. **424**, 175 (2006).

[6] A. Barrat, M. Barthélemy, and A. Vespignani, *Dynamical Processes on Complex Networks* (Cambridge University Press, Cambridge, England, 2008).

[7] D. J. Watts and S. H. Strogatz, Nature (London) **393**, 440 (1998).

[8] A.-L. Barabási and R. Albert, Science **286**, 509 (1999).

[9] C. Song, S. Havlin, and H. A. Makse, Nature (London) **433**, 392 (2005).

[10] H. E. Stanley, *Introduction to Phase Transitions and Critical Phenomena* (Oxford University Press, Oxford, 1971).

[11] J. Cardy, *Scaling and Renormalization in Statistical Physics* (Cambridge University Press, Cambridge, England, 1996).

[12] S. H. Yook, F. Radicchi, and H. Meyer-Ortmanns, Phys. Rev. E **72**, 045105(R) (2005).

[13] C. Song, S. Havlin, and H. A. Makse, Nat. Phys. **2**, 275 (2006).

[14] K.-I. Goh, G. Salvi, B. Kahng, and D. Kim, Phys. Rev. Lett. **96**, 018701 (2006).

[15] C. Song, L. K. Gallos, S. Havlin, and H. A. Makse, J. Stat. Mech.: Theory Exp. 2007, P03006 (2007).

[16] J. S. Kim, K.-I. Goh, G. Salvi, E. Oh, B. Kahng, and D. Kim, Phys. Rev. E **75**, 016110 (2007).

[17] J. S. Kim, K.-I. Goh, B. Kahng, and D. Kim, Chaos **17**, 026116 (2007).

[18] J. S. Kim, K.-I. Goh, B. Kahng, and D. Kim, New J. Phys. **9**, 177 (2007).

[19] H. D. Rozenfeld, L. K. Gallos, C. Song, and H. A. Makse, arXiv:0808.2206.

[20] F. Radicchi, J. J. Ramasco, A. Barrat, and S. Fortunato, Phys. Rev. Lett. **101**, 148701 (2008).

[21] B. Bollobás, *Modern Graph Theory* (Springer-Verlag, New York, 1998).

[22] B. B. Mandelbrot, *The Fractal Geometry of Nature* (W. H. Freeman, New York, 1982).

[23] I. Derényi, G. Palla, and T. Vicsek, Phys. Rev. Lett. **94**, 160202 (2005).

[24] P. Erdös and A. Rényi, Publ. Math. (Debrecen) **6**, 290 (1959).

[25] S. N. Dorogovtsev, J. F. F. Mendes, and A. N. Samukhin, Phys. Rev. Lett. **85**, 4633 (2000).

[26] R. Albert, H. Jeong, and A.-L. Barabási, Nature (London) **401**, 130 (1999).

[27] E. Ravasz and A.-L. Barabási, Phys. Rev. E **67**, 026112 (2003).

[28] J. S. Andrade, H. J. Herrmann, R. F. S. Andrade, and L. R. da Silva, Phys. Rev. Lett. **94**, 018702 (2005).

[29] K. Ichikawa, M. Uchida, M. Tsuru, and Y. Oie, arXiv:0808.0053.

[30] M. E. J. Newman, Proc. Natl. Acad. Sci. U.S.A. **98**, 404 (2001).

[31] V. Colizza, A. Flammini, A. Maritan, and A. Vespignani, Physica A **352**, 1 (2005).

[32] www.imdb.com